

Supporting Information

One-pot Single-step Copolymerization of Aromatic Trifluorovinyl Ethers toward Perfluorocyclobutyl (PFCB) Segmented Copolymers

*Jiyoung Park, Tugba G Kucukkal, Jung-Min Oh, Steven J Stuart, Stephen E. Creager, Gustavo Muñoz, and Dennis W. Smith Jr.**

Department of Chemistry, Clemson University, Clemson, South Carolina 29634, United States

*Department of Chemistry, Mississippi State University, Mississippi State, MS, 39762

Table of Contents

1. Materials	S 2
2. Instrumentations	S 2
3. Preparation and characterization of copolymers	S 3-4
Preparation of polymers (Scheme S1)	S 5
¹ H and ¹⁹ F NMR spectra of polymers (Fig.S1- Fig.S3)	S 5-7
Illustration and rationalization of copolymer formations (Scheme S2-S3)	S 8-9
TGA and DSC of polymers (Fig.S4- Fig.S5)	S 10
¹ H NMR spectra of sulfonated polymers (Fig.S6)	S11
4. Computational Study Details	S 12
Computational data: Ea with different DFT methods (Table S1)	S12
Energy State Diagrams of TFVE Dimerizations (Scheme S4)	S 13
Optimized TS Structures of PFCB Model Compounds (Fig.S7)	S 14
Computational data: Geometries and Energies of TS (Table S2-S3)	S 14-15
References	S16

Experimental Details

1. Materials

Chlorosulfonic acid (CSA) was purchased from Alfa Aesar. Commercially available monomers, 4,4'-bis(4-trifluorovinyloxy)biphenyl (BP) and 2,2'-bis(4-trifluorovinyloxy) biphenyl-1,1,1,3,3,3-hexafluoropropane (6F) and their oligomers (BPo and 6Fo) were kindly donated by Tetramer Technologies, L.L.C. 6F monomer was purified by column with hexane before use. All other chemicals and solvents were obtained from Aldrich and used as received unless stated otherwise.

2. Instrumentations

^1H and ^{19}F NMR spectra were recorded on a JEOL Eclipse + 300 with 15s relaxation times (T_1). Gel permeation chromatography (GPC) data were collected in CHCl_3 from a Waters 2690 Alliance System with photodiode array detection. Molecular weights were obtained using polystyrene as a standard. Elemental microanalysis data for carbon, hydrogen, and fluorine were obtained from Atlantic Microlab, Inc. (Norcross, GA). Thermal gravimetric analysis (TGA) was performed on a Mettler-Toledo 851 instrument in nitrogen and air at a heating rate of 10 °C/min up to 800 °C. Differential scanning calorimetry (DSC) analysis was performed on a TA Q1000 instrument in nitrogen at a heating rate of 10 °C/min up to 200 °C. The glass transition temperature (T_g) of PFCB copolymers was obtained from a second heating cycle using TA Universal Analysis 2000 software suite.

3. Preparation and characterization of copolymers and sulfonated copolymers

3.1. Synthesis of PFCB1 (Copolymerization of BPo with 6Fo.)

Synthesis of copolymer PFCB1 was conducted as follows: 5g of BP oligomer (BP_o) and 5g of 6F oligomer (6F_o, Mn= 15,000 g/mol), 10 mL of diphenylether were added to three-neck 250 mL flask, equipped with a condenser, argon inlet and a mechanical stirrer. The reaction mixture was slightly heated at 60 °C and the melted system was sparged with argon gas for 30 min. The thermal step-growth cyclopolymerization was conducted at 140 °C for 24 h, 160 °C for 72 h, 180 °C for 24 h, and 210 °C for 14 h under argon blanket. The resulting viscous crude polymer was cool down and dissolved in tetrahydrofuran (THF). The solution was precipitated from a large excess of methanol. The resulting off-white fibrous copolymer was extracted via soxhlet extractor with methanol for 24 h to remove diphenylether and unreacted monomers. The copolymer was dried at 60 °C in vacuum for 24 h. Yield: 60%, ¹H NMR (300 MHz, CDCl₃) δ 7.47 (d, J = 9 Hz, H_f'), 7.40–7.30 (m, H_g'), 7.30–7.20 (m, overlapped by H_e' and CDCl₃), 7.07 (d, J = 6 Hz, H_h'); ¹⁹F NMR (283 MHz, CDCl₃) δ -64 (s, F_d'), -126 – (-133) (m, the overlap of cyclobutyl-F₆ on BP and 6F segments). Elemental Analysis: Found: C, 51.47; H, 1.89; F, 38.57.

3.2. Synthesis of PFCB2 (Copolymerization of BP_o with 6F_m.)

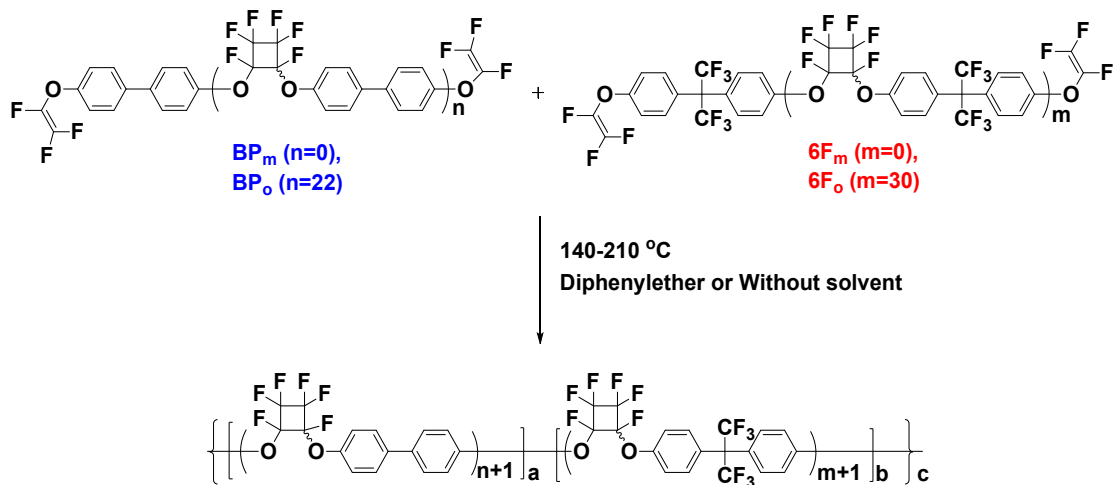
A segmented copolymer PFCB2 of BP oligomer (BP_o, Mn= 8,000 g/mol, 10g), 6F monomer (6F_m, 10g), was prepared using the same synthesis and purification routine of polymer PFCB1. Yield: 80-85%, ¹H NMR (300 MHz, CDCl₃) δ 7.47 (d, J = 9 Hz, H_f'), 7.40–7.30 (m, H_g'), 7.30–7.20 (m, overlapped by H_e' and CDCl₃), 7.07 (d, J = 6 Hz, H_h'); ¹⁹F NMR (283 MHz, CDCl₃) δ -64 (s, F_d'), -126 – (-133) (m, the overlap of cyclobutyl-F₆ on BP and 6F segments). Elemental Analysis: Found: C, 50.59; H, 1.94; F, 40.08.

3.3. Synthesis of PFCB3 (Copolymerization of BP_m with 6F_m.)

A copolymer of BPm and 6Fm was also synthesized without solvent, diphenylether, at 140 °C for 24 h, 160 °C for 48 h, 180 °C for 24 h with argon inlet. The resulting viscous copolymer was cooled down and dissolved in THF. The solution was precipitated in a methanol and the resulting off-white fibrous copolymer was purified in a soxhlet extractor with methanol for 24 h. The copolymer was dried at 60 °C in vacuum for 24 h. Yield: 85%, ^1H NMR (300 MHz, CDCl_3) δ 7.47 (d, $J = 9$ Hz, H_f), 7.40–7.30 (m, H_g), 7.30–7.20 (m, overlapped by H_e and CDCl_3), 7.07 (d, $J = 6$ Hz, H_h); ^{19}F NMR (283 MHz, CDCl_3) δ -64 (s, F_d), -126 – (-133) (m, the overlap of cyclobutyl- F_6 on BP and 6F segments). Elemental Analysis: Found: C, 50.27; H, 1.83; F, 40.23.

3.4. Sulfonation of PFCB aryl ether copolymers, PFCB2 and PFCB3.

Five grams of PFCB2 aryl ether copolymer was dissolved in 100 mL of dichloromethane (DCM). The chlorosulfonic acid (CSA) was added at 36 °C internal temperature and then the mixture was stirred vigorously for 1 h at the same temperature. The various degree of sulfonation was obtained by controlling the equivalent of chlorosulfonic acid (Sample No: weight ratio CSA (g)/Polymers(g), sPFCB2-1: 1.5/1, sPFCB2-2: 2.0/1, sPFCB2-3: 2.5/1, sPFCB3: 2.5/1). The precipitate, being sPFCB, was recovered by decanting DCM into a crushed ice and then washed in cold and boiling deionized water several times to remove excess acids. The supernatant has been removed and the final precipitate was recovered by filtration and dried in a vacuum oven for 24 h at 60 °C. Yield: 90-97%, ^1H NMR (300 MHz, $\text{DMSO}-d_6$) δ 8.05 (s, br, H_e), 7.70 (s, br, H_b), 7.50 (s, br, H_d), 7.35 (s, br, H_a), 7.20 (s, br, H_c); ^{19}F NMR (283 MHz, $\text{DMSO}-d_6$) δ -63 (s, $-\text{CF}_3$, 6F), -94–(-140) (m, br, the overlap of cyclobutyl- F_6 on BP and 6F).



Copolymers

PFCB1 = Copolymer of BP_o and 6F_o

PFCB2 = Copolymer of BP_o and 6F_m

PFCB3 = Copolymer of BP_m and 6F_m

Scheme S1. Preparation of PFCB Aryl Ether Copolymers; BP_m, BP_o, 6F_m, and 6F_o refer to BP monomer, BP oligomer, 6F monomer, and 6F oligomer, respectively.

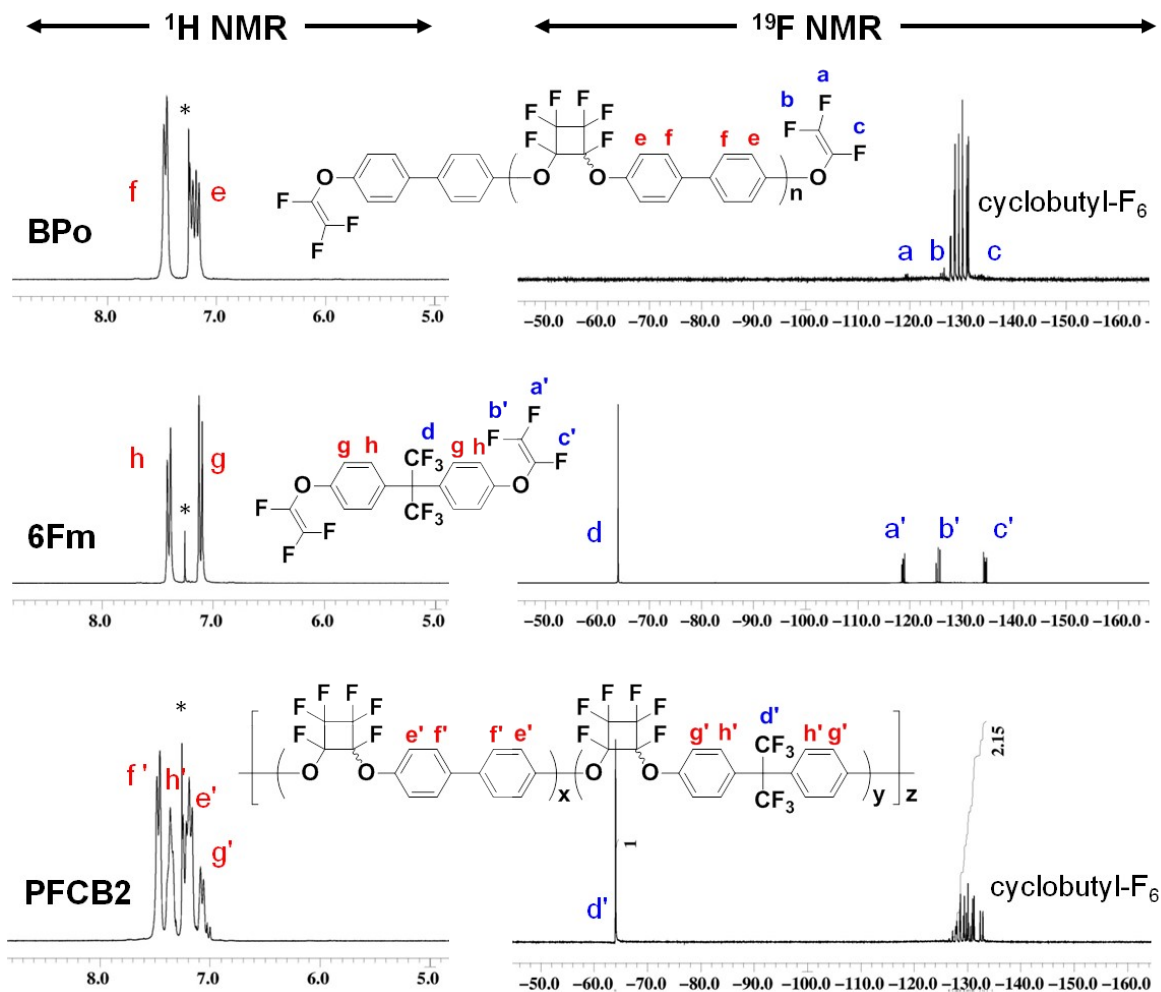


Figure S1. ^1H NMR (in CDCl_3^* , left) and ^{19}F NMR (in CDCl_3^* , right) spectra of **BP oligomer** (BPO), **6F monomer** (6Fm), and **PFCB2** (BPo-co-6Fm) copolymer.

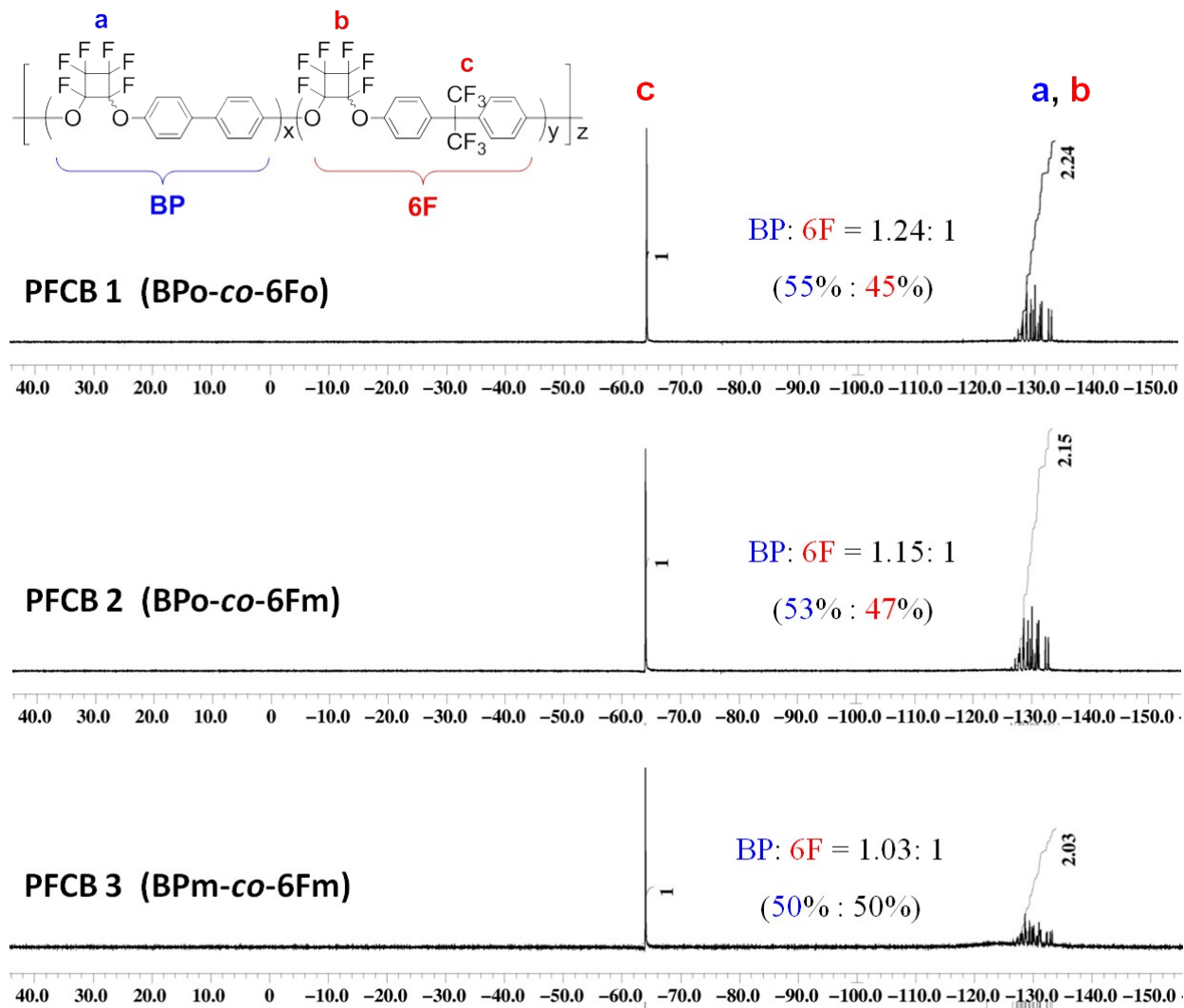


Figure S2. ^{19}F NMR (in CDCl_3) spectra of (a) **PFCB1** (BPO-co-6Fo), (b) **PFCB2** (BPO-co-6Fm), and (c) **PFCB3** (BPM-co-6Fm) copolymers with their compositional ratios of the BP and 6F repeat unit in the copolymer chains.

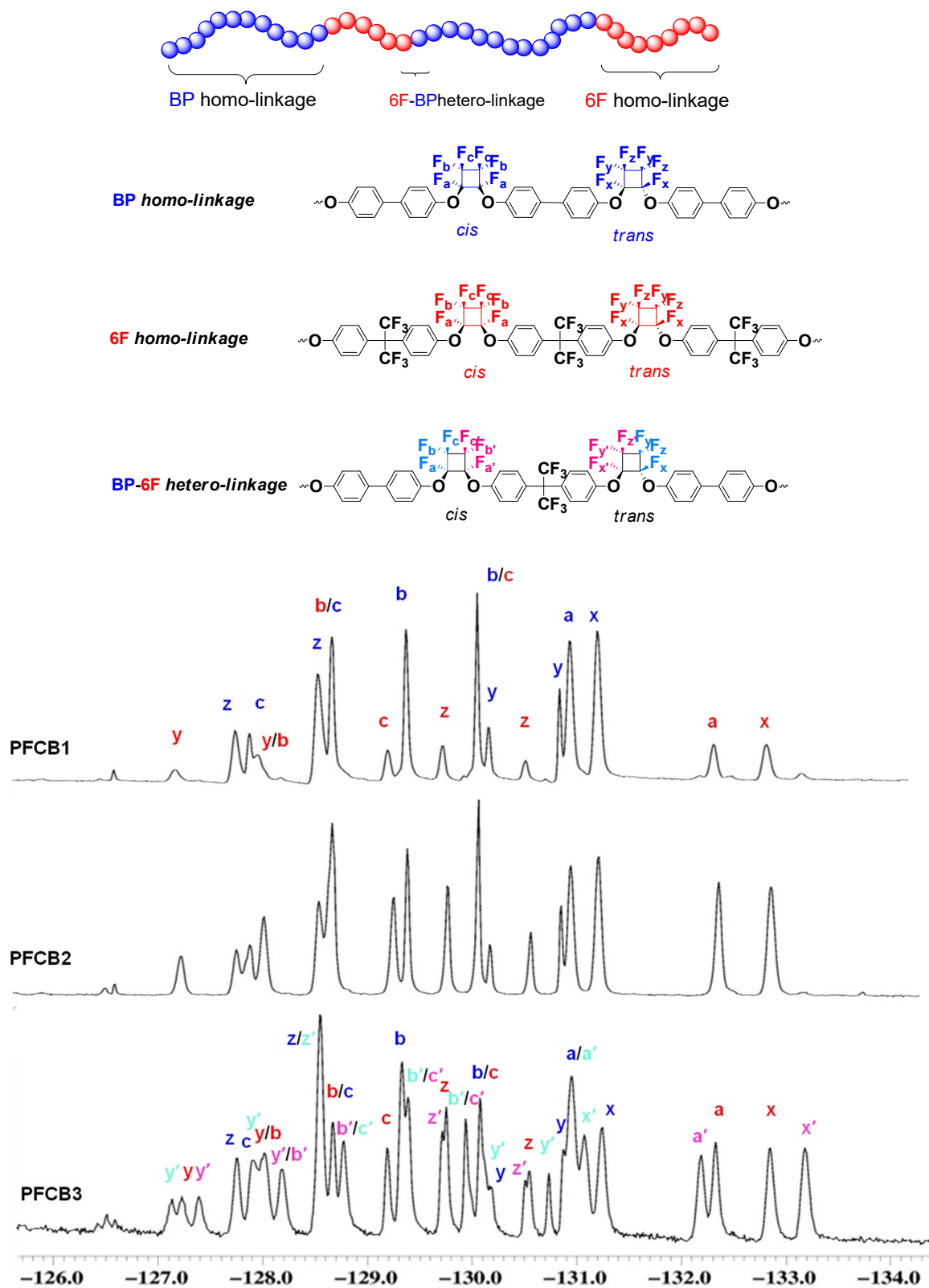
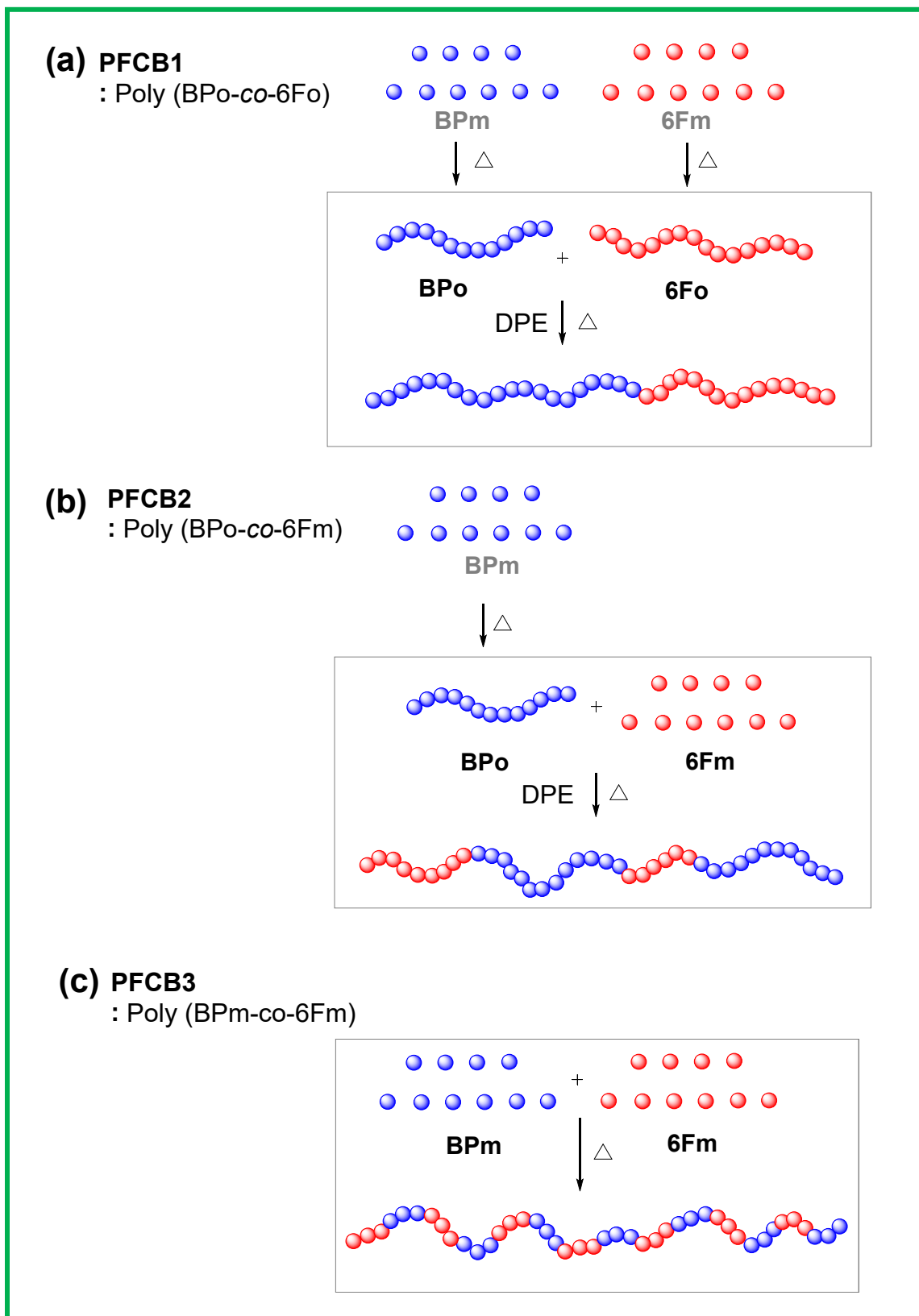
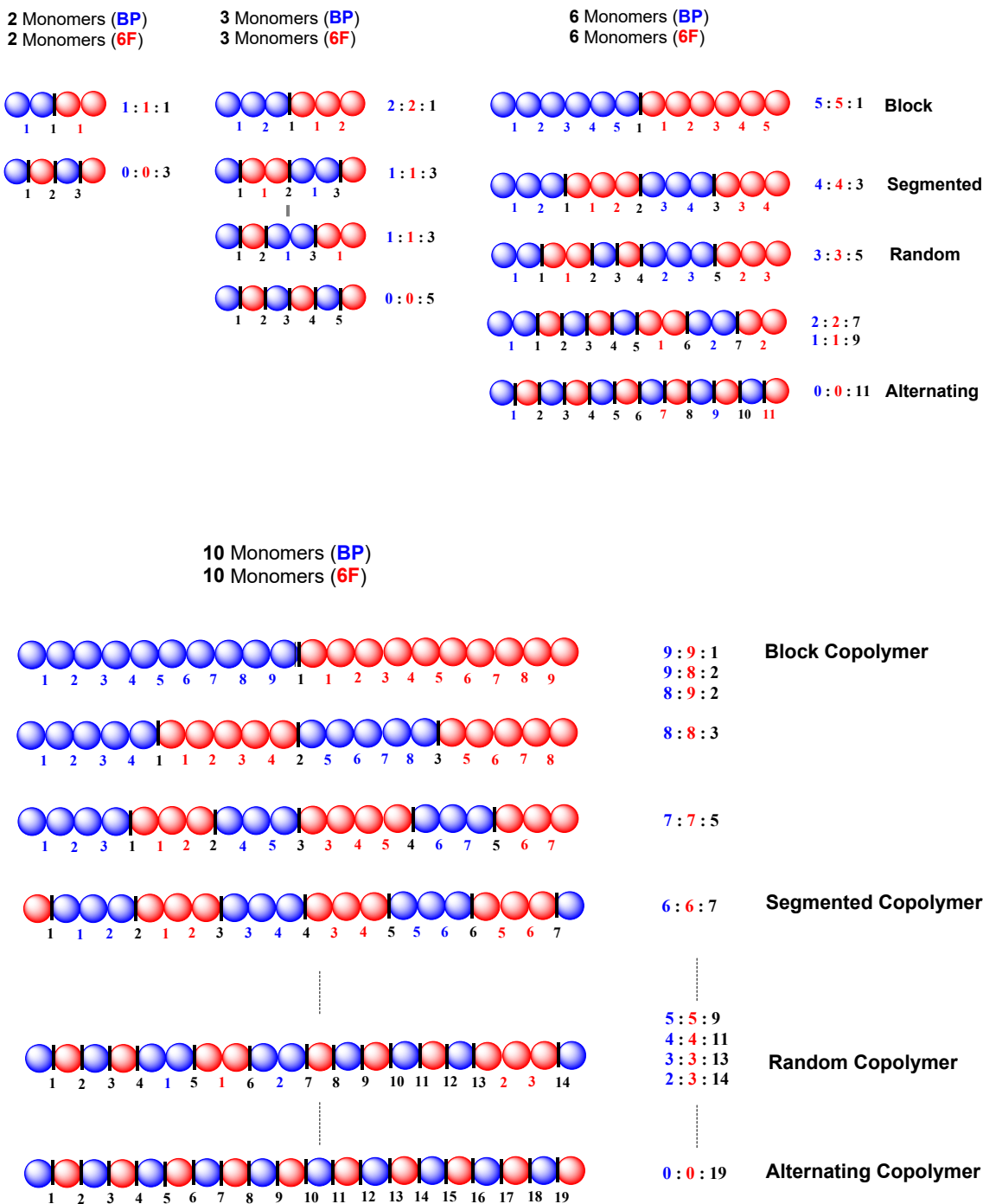


Figure S3. ^{19}F NMR (in CDCl_3^* , right) spectra of (a) **PFCB1** (BPo-co-6Fo), (b) **PFCB2** (BPo-co-6Fm), and (c) **PFCB3** (Bpm-co-6Fm) copolymers.



Scheme S2. Illustration of copolymer formations: (a) PFCB1, (b) PFCB2, and (c) PFCB3 segmented copolymer.



Scheme S3. Rationalization of copolymer types along with ratios of BP homo-linkage, 6F homo-linkage, and BP-6F hetero-linkage: Block, Segmented, Random, and Alternating Copolymer.

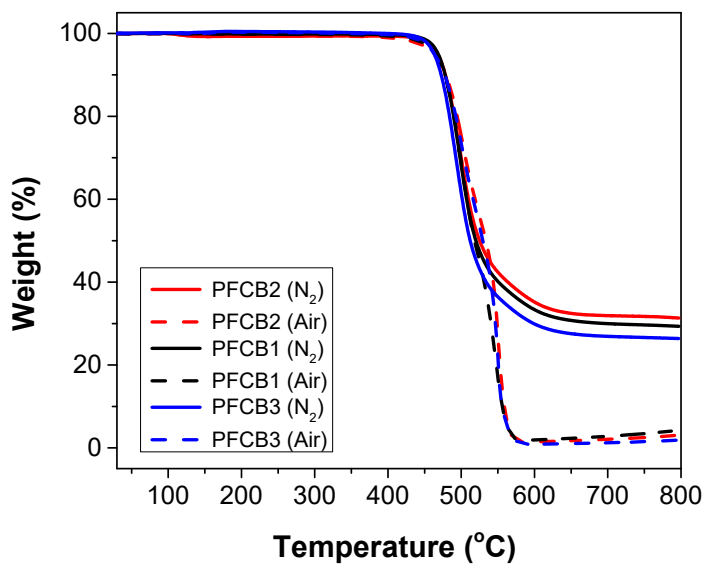


Figure S4. TGA curves of PFCB copolymers.

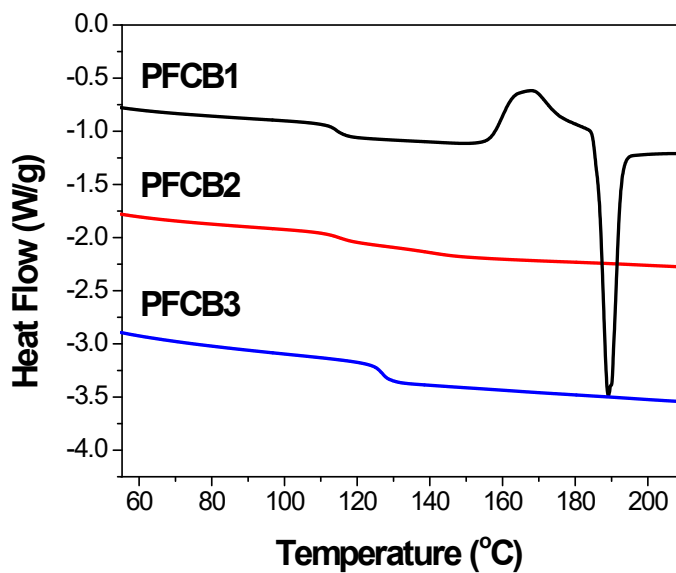


Figure S5. DSC thermogram of PFCB copolymers.

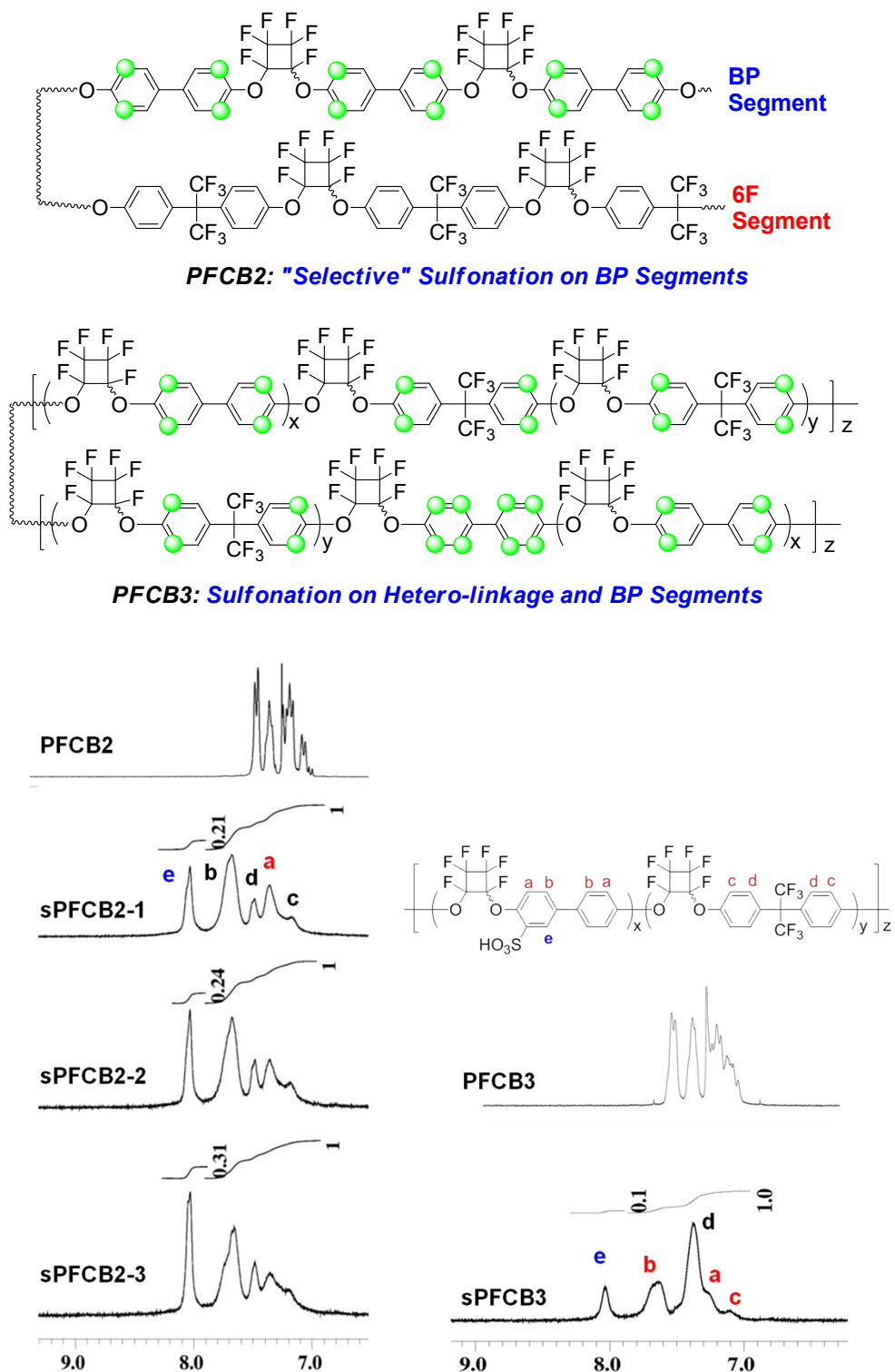


Figure S6. ¹H NMR (in DMSO) spectra of PFCB copolymers: **PFCB 2** (BPo-co-6Fm) and **PFCB3** (BPM-co-6Fm) and their sulfonated copolymers: **sPFCB2-1**, **sPFCB2-2**, **sPFCB2-3**, and **sPFCB3**.

4. Computational Details

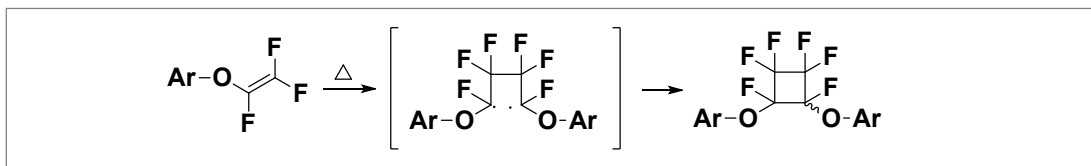
All calculations were performed using the Gaussian 09 software [1]. The transition state structures were located at the B3LYP/6-31G(d) level of theory at singlet state (singlet transition states were found to have lower energy than the triplet). Presence of only one imaginary frequency was confirmed by frequency calculations and the vibrational frequencies were visualized using the Avogadro software [2] to ensure that the imaginary frequency motion corresponds to the Carbon-Carbon (C2-C2) bond formation. Finally, the single point energy calculations were performed on the B3LYP/6-31G(d) optimized transition state structures at five different levels of theory: B3LYP/6-31+G(d), B3LYP/6-311++G(d,p), mPW1PW91/6-31+G(d,p), ω B97X/cc-pVTZ and M062X/6-31+G(d,p). The reactant, intermediate, and product structures were optimized using the aforementioned five methods.

Table S1. Computational Data: E_a for S11, S12, and S22 with different DFT methods.

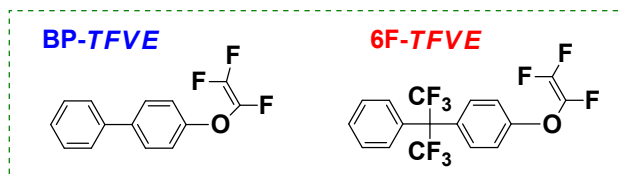
	E_a (kcal/mol)				
	B3LYP/ 6-31+G(d)	B3LYP/ 6-311++G(d,p)	mPW1PW91/ 6-31G+(d,p)	ω B97X/ cc-VTZ	M062X/ 6-31+G(d,p)
S11 (S1 + S1) ^a	28.0	29.9	27.3	39.9	28.0
S12 (S1 + S2) ^b	28.1	30.0	27.5	40.1	28.5
S22 (S2 + S2) ^c	43.4	40.2	43.5	57.3	46.0

^a Homo-dimerizations of S1 small molecule (BP-TFVE), ^b Co-dimerizations of S1 and S2 small molecules (BP-TFVE and 6F-TFVE), and ^c Homo-dimerizations of S2 small molecule (6F-TFVE). S1 and S2 small molecule structures are illustrated in Scheme S4.

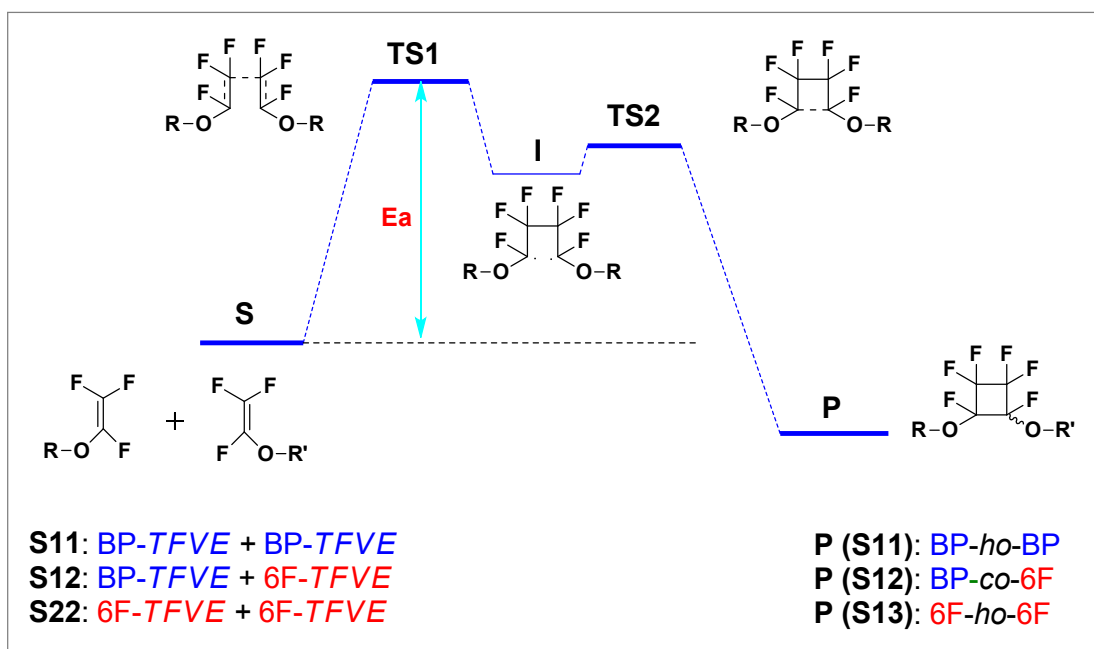
(i) [2 + 2] cyclodimerization of monofunctional arylTFVE



Model Compounds



(ii) Energy state diagram of dimerizations



Scheme S4. Energy state diagrams for homo-dimerizations and co-dimerizations of aryl TFVE small molecules.

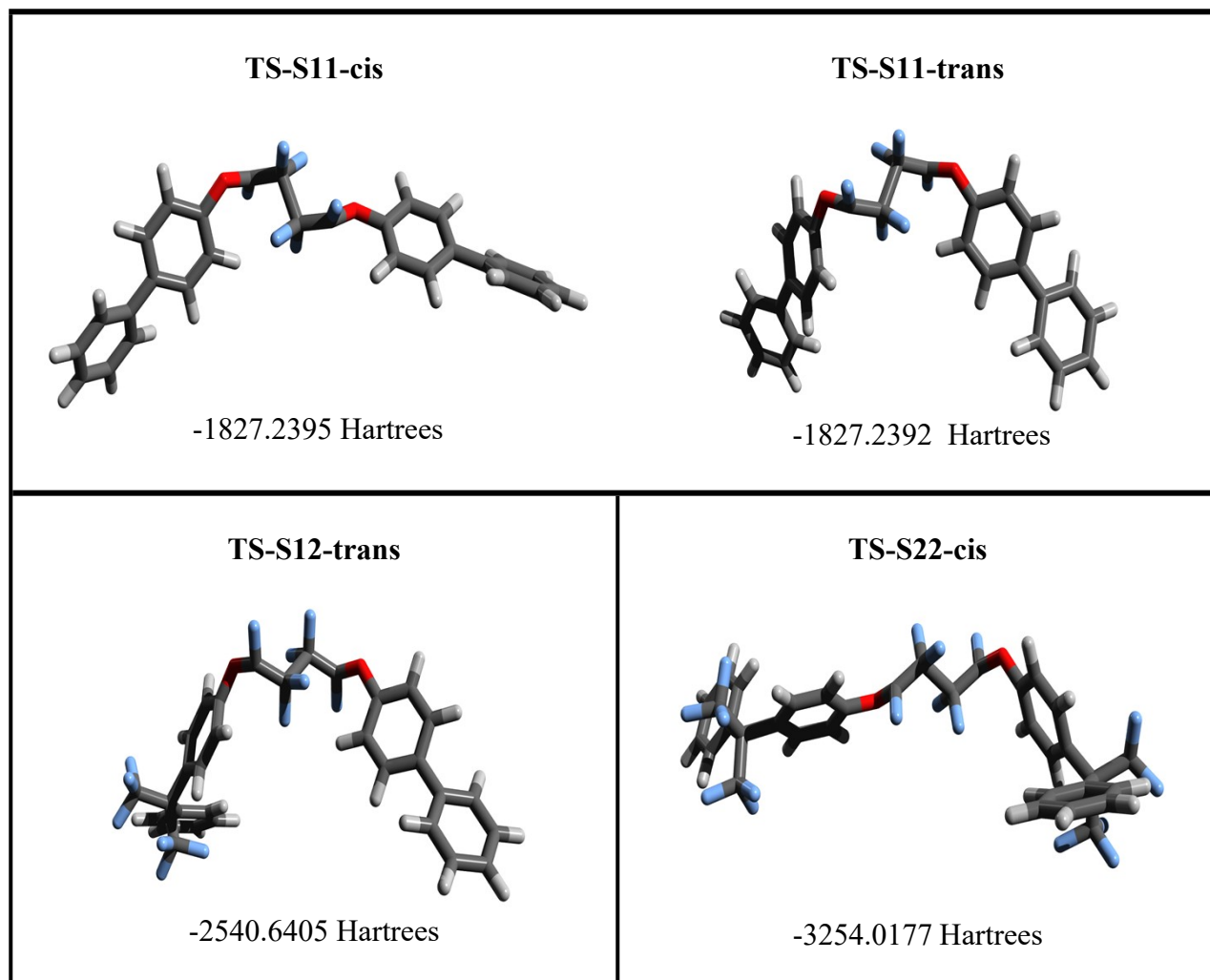


Figure S7. Optimized transition state structures for S11, S12 and S22.

Table S2. Computational Data: Geometries of TS-S11, TS-S12 and TS-S22.

	Bond Length (Å)		Angle (°)	
	C1-C2 (C3-C4)	C2-C3	C1-C2-C3 (C2-C3-C4)	C1-C2-C3-C4
TS-S11- <i>cis</i>	1.42 (1.41)	1.78	111.6 (113.1)	-179.5
TS-S11- <i>trans</i>	1.42 (1.41)	1.78	113.0 (111.8)	-178.7
TS-S12- <i>trans</i>	1.42 (1.41)	1.79	113.0 (111.3)	-179.2
TS-S22- <i>cis</i>	1.41 (1.42)	1.79	112.0 (111.6)	-177.8

Table S3. Computational Data: Energies (Hartrees) of Reactants, Products and Transition States at the B3LYP/6-31+G(d) level of theory.

	Reactant	TS	Product
S11 (S1 + S1) ^a	-1827.2836	-1827.2395 (<i>cis</i>) -1827.2392 (<i>trans</i>)	-1827.3423 (<i>cis</i>) -1827.3437 (<i>trans</i>)
S12 (S1 + S2) ^b	-2540.6851	-2540.6405 (<i>trans</i>)	-2540.7439 (<i>cis</i>) -2540.7451 (<i>trans</i>)
S22 (S2 + S2) ^c	-3254.0866	-3254.0177 (<i>cis</i>)	-3254.1451 (<i>cis</i>) -3254.1464 (<i>trans</i>)

^a Homo-dimerization of S1 small molecule (BP-TFVE), ^b Co-dimerization of S1 and S2 small molecules (BP-TFVE and 6F-TFVE), and ^c Homo-dimerization of S2 small molecule (6F-TFVE). S1 and S2 small molecule structures are illustrated in Scheme S4.

References

1. Gaussian 09, Revision D.01, M. J. Frisch, G. W. Trucks, H. B. Schlegel, G. E. Scuseria, M. A. Robb, J. R. Cheeseman, G. Scalmani, V. Barone, B. Mennucci, G. A. Petersson, H. Nakatsuji, M. Caricato, X. Li, H. P. Hratchian, A. F. Izmaylov, J. Bloino, G. Zheng, J. L. Sonnenberg, M. Hada, M. Ehara, K. Toyota, R. Fukuda, J. Hasegawa, M. Ishida, T. Nakajima, Y. Honda, O. Kitao, H. Nakai, T. Vreven, J. A. Montgomery, Jr., J. E. Peralta, F. Ogliaro, M. Bearpark, J. J. Heyd, E. Brothers, K. N. Kudin, V. N. Staroverov, R. Kobayashi, J. Normand, K. Raghavachari, A. Rendell, J. C. Burant, S. S. Iyengar, J. Tomasi, M. Cossi, N. Rega, J. M. Millam, M. Klene, J. E. Knox, J. B. Cross, V. Bakken, C. Adamo, J. Jaramillo, R. Gomperts, R. E. Stratmann, O. Yazyev, A. J. Austin, R. Cammi, C. Pomelli, J. W. Ochterski, R. L. Martin, K. Morokuma, V. G. Zakrzewski, G. A. Voth, P. Salvador, J. J. Dannenberg, S. Dapprich, A. D. Daniels, Ö. Farkas, J. B. Foresman, J. V. Ortiz, J. Cioslowski, and D. J. Fox, Gaussian, Inc., Wallingford CT, 2009.
2. M. D Hanwell, D. E. Curtis, D. C. Lonie, T. Vandermeersch, E. Zurek, and G. R. Hutchison "Avogadro: an advanced semantic chemical editor, visualization, and analysis platform." *Journal of Cheminformatics*, **4** (2012) 17 <http://avogadro.openmolecules.net/>